DISTILLHGNN: A KNOWLEDGE DISTILLATION APPROACH FOR HIGH-SPEED HYPERGRAPH NEURAL NETWORKS

Anonymous authors
Paper under double-blind review

ABSTRACT

This paper introduces a novel framework designed to significantly enhance the inference speed and memory efficiency of Hypergraph Neural Networks (HGNNs) while maintaining their high accuracy. Our approach, named DistillHGNN, employs an advanced teacher-student knowledge distillation strategy, where the teacher model comprises an HGNN and a Multi-Layer Perceptron (MLP). In this setup, the HGNN generates embeddings, which the MLP subsequently processes to predict soft labels. The student model consists of a lightweight Graph Convolutional Network (GCN), TinyGCN, paired with an MLP and optimized for online prediction. We leverage contrastive learning to train both TinyGCN and HGNN simultaneously, facilitating the transfer of high-order and structural knowledge from the HGNN to the TinyGCN. Additionally, the teacher employs a mechanism to transfer knowledge to the student model through soft labels. This dual transfer mechanism enables the student to effectively capture complex dependencies while benefiting from the lightweight GCN's faster inference and lower computational cost. The student is trained using both labeled data and soft labels provided by the teacher, with contrastive learning further ensuring that the student retains high-order relationships. This makes the proposed method efficient and suitable for real-time applications, achieving performance comparable to traditional HGNNs but with significantly reduced resource requirements. Experimental results on several real-world datasets demonstrate that our method significantly reduces inference time while maintaining accuracy comparable to HGNN, and it achieves higher accuracy than state-of-the-art techniques, like LightHGNN, with a similar inference time.

1 INTRODUCTION

Hypergraphs, with their ability to capture multi-node relationships through degree-free hyperedges, offer a significant advantage over traditional graphs in modeling complex high-order interactions Fan et al. (2021). As a result, several Hypergraph Neural Networks (HGNNs) have been developed to tackle various tasks, such as node classification in citation networks, recommendation in bipartite graphs, and link prediction in biological networks ZENG et al. (2024). Despite these advances, the widespread adoption of HGNNs in large-scale industrial applications still needs to be improved. This is primarily due to the heavy reliance on hypergraph structures during inference, which requires substantial memory and computational resources Yu et al. (2024). As the hypergraph size and the HGNNs' depth increase, the inference time and memory requirements grow exponentially, posing significant challenges for their deployment in real-world scenarios where speed and efficiency are crucial Feng et al. (2024). This disparity highlights the need for more lightweight and scalable solutions that can harness the representational power of HGNNs while being suitable for high-speed, resource-constrained environments.

The dependency of HGNNs on the hypergraph structure arises from their message-passing mechanism, which involves complex high-order interactions between vertices and hyperedges. To address this challenge, recent methods like Graph-Less Neural Networks (GLNN) Zhang et al. (2021), and Noise-robust Structure-aware MLPs On Graphs (NOSMOG) Tian et al. (2022) and Knowledge-inspired Reliable Distillation (KRD)Wu et al. (2023) have aimed to eliminate graph dependencies

by distilling knowledge from GNNs to MLPs. However, these methods focus on simple graph structures, using soft labels or pairwise edge information as supervision, and are insufficient for hypergraphs, where hyperedges connect multiple vertices, leading to more intricate neighborhoods. Consequently, MLPs, despite their scalability and graph independence, often underperform on hypergraph data, showing an average decline in accuracy compared to HGNNs. Recently, LightHGNN has extended the GLNN framework to hypergraphs by distilling knowledge from HGNNs into MLPs using soft labels. While this method effectively transfers class information, it cannot convey the complex high-order relationships and structural knowledge inherent in hypergraphs. Soft labels alone are insufficient to capture these intricate dependencies. This limitation raises an important question: *Can we develop a strategy that distills soft labels and transfer the hypergraph's structural and high-order knowledge to the student model, ensuring a more comprehensive knowledge transfer*?

Present work. In this paper, we present DistillHGNN, a novel framework that significantly improves the inference speed and memory efficiency of HGNNs while maintaining high accuracy. DistillHGNN leverages a comprehensive teacher-student knowledge distillation approach. The teacher model includes an HGNN and an MLP, where the HGNN captures complex relationships within the hypergraph and generates node embeddings. These embeddings are then passed to the MLP, which produces soft labels. Together, these embeddings and soft labels form the knowledge to be transferred to the student model. The student model includes a lightweight GCN called TinyGCN and an MLP. TinyGCN, designed for efficient learning, consists of a single-layer GCN without non-linear activation functions to reduce computational complexity. A contrastive learning strategy maximizes the similarity between the embeddings generated by the HGNN and TinyGCN, effectively transferring high-order structural knowledge to the student model. This strategy enables TinyGCN to replicate the behavior of the HGNN while operating at a significantly lower computational cost. Moreover, soft labels are transferred as supplementary labeled data, further using the training process of the student model. This dual transfer mechanism allows the TinyGCN and MLP in the student model to inherit both high-order dependencies and structural knowledge from the HGNN, resulting in faster inference and improved performance. Novelties of the Proposed Method are:

1. DistillHGNN transfers soft labels and structural knowledge from HGNN to TinyGCN, resulting in richer and more effective knowledge distillation than methods like LightHGNN.
2. DistillHGNN utilizes a contrastive learning strategy to maximize the similarity between embeddings generated by the HGNN and TinyGCN, effectively transferring high-order structural knowledge to the student model.
3. TinyGCN is streamlined to a single layer without activation functions, reducing computational complexity while effectively capturing the high-order relationships of the teacher HGNN.
4. The proposed method achieves inference speeds comparable to LightHGNNFeng et al. (2024) but with higher accuracy, making it highly suitable for real-time and large-scale applications.
5. By integrating the representational power of HGNNs with the lightweight nature of TinyGCN, DistillHGNN delivers fast and accurate predictions while maintaining low memory and computational requirements.

2 PRELIMINARIES

Graph and Hypergraph: A graph $G = (V, E)$ consists of a set of nodes V and edges E, where each edge $e = (v_i, v_j)$ connects two nodes, v_i and v_j. The structure of a graph can be represented by its adjacency matrix $A \in \mathbb{R}^{n \times n}$, where $A_{ij} = 1$ if there is an edge between nodes v_i and v_j, and 0 otherwise. This representation is limited to pairwise relationships between nodes. A hypergraph $\mathcal{H} = (V, E)$, on the other hand, generalizes the concept of a graph by allowing hyperedges $e \in E$ to connect any subset of nodes, enabling the representation of complex, multi-node relationships. A hypergraph is represented by its incidence matrix $\mathcal{H} \in \mathbb{R}^{n \times m}$, where n is the number of nodes, m is the number of hyperedges, and $\mathcal{H}_{ij} = 1$ if node v_i is connected to hyperedge e_j, and 0 otherwise. This matrix effectively captures high-order interactions among nodes, making it suitable for modeling heterogeneous graphs. To convert a hypergraph into a homogeneous graph, we can

compute a projected adjacency matrix $A \in \mathbb{R}^{n \times n}$ as $A = HW\mathcal{H}^\top - D_v$, where $W \in \mathbb{R}^{m \times m}$ is the hyperedge weight matrix, and D_v is the diagonal node degree matrix, with $D_v(i,i) = \sum_{j=1}^{m} \mathcal{H}_{ij}$. This transformation reduces the hypergraph to a traditional graph where two nodes are connected if they share common hyperedges.

Graph Convolutional Networks (GCNs) Kipf & Welling (2016) are designed to operate directly on graph-structured data, allowing for effective representation learning from the connections between nodes. In the context of a graph, the input consists of an adjacency matrix A that encodes the relationships between nodes and a feature matrix X that contains the features of each node. The fundamental operation in a GCN is performed through a series of graph convolutional layers. The update rule for node embeddings at layer l is defined as:

$$H^{(l+1)} = \sigma(\tilde{A}H^{(l)}W^{(l)}) \tag{1}$$

where $H^{(l)}$ represents the node embeddings at layer l (for layer 0, $H^{(0)}$ is the input feature matrix), $W^{(l)}$ is the trainable weight matrix at layer l, σ is a non-linear activation function (e.g., ReLU), and $\tilde{A}$ is the normalized adjacency matrix defined as:

$$\tilde{A} = \hat{D}^{-1/2}\hat{A}\hat{D}^{-1/2} \tag{2}$$

Here, $\hat{A} = A + I$ is the adjacency matrix with self-loops (adding the identity matrix I to include each node's feature in the aggregation), and $\hat{D}$ is the degree matrix of $\hat{A}$, where $\hat{D}_{ii} = \sum_j \hat{A}_{ij}$. The term $\hat{D}^{-1/2}$ represents the normalized degree matrix (the square root inverse of the degree matrix). This normalization ensures the node features are scaled properly, preventing exploding or vanishing gradients during training.

Hypergraph Neural Network (HGNN) is a powerful extension of the GCN designed to capture high-order relationships among nodes by leveraging the structure of hypergraphs. In a hypergraph $\mathcal{H} = (V, E)$, each hyperedge $e_j \in E$ can connect multiple nodes from the set V, allowing for more complex interactions than simple pairwise connections. The incidence matrix $\mathcal{H} \in \mathbb{R}^{n \times m}$ represents these connections, where $\mathcal{H}_{ij} = 1$ if node v_i is connected to hyperedge e_j. HGNNs use the hypergraph Laplacian, derived from the node degree matrix D_v and the hyperedge degree matrix D_e, to propagate information across the hypergraph. This is achieved through a message-passing mechanism that updates node features using the formula:

$$H^{(l+1)} = \sigma\left(D_v^{-1/2}\mathcal{H}WD_e^{-1}\mathcal{H}^T D_v^{-1/2}H^{(l)}\Theta^{(l)}\right) \tag{3}$$

where $\Theta^{(l)}$ represents the learnable weights and $\sigma(\cdot)$ is a non-linear activation function. This formulation allows HGNNs to effectively aggregate and propagate features, accounting for the structure of the hypergraph, thus enabling the modeling of complex dependencies between nodes. HGNNs have demonstrated their versatility and effectiveness in various applications, including recommendation systems, social networks, and biological data analysis Feng et al. (2019).

3 METHODOLOGY

The overall architecture of the proposed DistillHGNN framework is shown in Figure 1.

The proposed method aims to enhance the inference speed and memory efficiency of HGNNs while maintaining performance comparable to HGNNs. The method is structured around a teacher-student knowledge distillation Figure 1. The teacher model is formed by an HGNN and a Multi-Layer Perceptron (MLP). The HGNN generates node embeddings $Z^t \in \mathbb{R}^{n \times d}$ by processing the node feature matrix $X \in \mathbb{R}^{n \times f}$ and the hypergraph incidence matrix $\mathcal{H} \in \mathbb{R}^{n \times m}$, where n is the number of nodes and m is the number of hyperedges. Given the node feature matrix $X \in \mathbb{R}^{n \times f}$, where f is the number of features, the HGNN propagates these features through the hypergraph structure using the hypergraph Laplacian:

$$L = D_v^{-1/2}\mathcal{H}WD_e^{-1}\mathcal{H}^T D_v^{-1/2} \tag{4}$$

Here, $D_v \in \mathbb{R}^{n \times n}$ is the diagonal node degree matrix, $D_e \in \mathbb{R}^{m \times m}$ is the diagonal hyperedge degree matrix, and $W \in \mathbb{R}^{m \times m}$ is the hyperedge weight matrix. The HGNN generates node embeddings $Z^t \in \mathbb{R}^{n \times d}$ by propagating the input features X through the Laplacian as:

$$Z^t = H^L \tag{5}$$

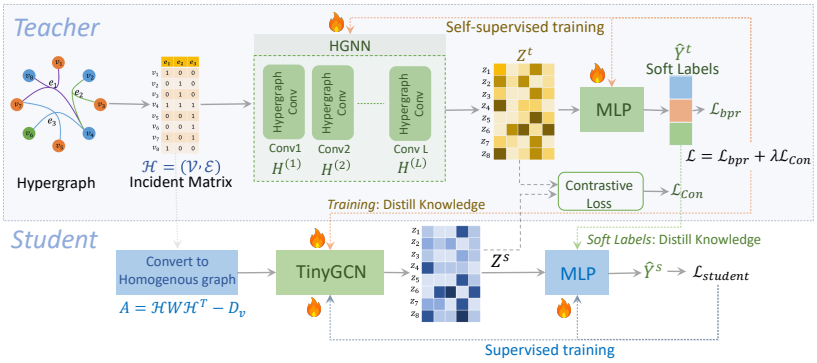

Figure 1: The proposed model consists of a teacher section (HGNN) and a student section (TinyGCN). The HGNN represents hypergraphs and generates soft labels using high-order relationships, while the TinyGCN captures direct neighborhood relations in graphs. Both models are trained using a supervised loss and contrastive loss to align their embeddings, enabling efficient knowledge distillation from teacher to student.

where L is the number of layers in the HGNN, and

$$H^{(l+1)} = \sigma\left(LH^{(l)}\Theta^{(l)}\right) \tag{6}$$

is the recursive update rule, with $H^{(l+1)} = \sigma\left(D_v^{-1/2}\mathcal{H}WD_e^{-1}\mathcal{H}^T D_v^{-1/2}H^{(l)}\Theta^{(l)}\right)$. The embedding Z^t is then input into the teacher MLP to predict soft labels Y^t. Let $C = \{c_1, c_2, \ldots, c_k\}$ be a set of node classes. A soft label is a vector with a length equal to the number of classes (i.e., $|C|$), where each value in the i-th cell represents the probability of the node belonging to the class $c_i \in C$. The supervised loss, called BPR loss, is defined as:

$$L_{\text{bpr}} = \frac{1}{|V^L|}\sum_{v\in V^L}\left(Y_v - Y_v^t\right)^2 \tag{7}$$

where Y_v is the true label for labeled nodes V^L, and Y_v^t is the soft label predicted for the node v.

To transfer knowledge from the teacher to the student model, we propose a lightweight GCN called TinyGCN, designed to mimic the embedding generation capabilities of HGNN. TinyGCN simplifies the standard GCN architecture by removing non-linear activation functions and using only a single layer. This minimalistic design allows TinyGCN to effectively capture the high-order relationships learned by the teacher model while significantly reducing inference time and computational complexity. In parallel, the graph is also passed through the TinyGCN to generate embeddings $Z^s \in \mathbb{R}^{n\times d}$ using the node feature matrix X and adjacency matrix $A^s \in \mathbb{R}^{n\times n}$ obtained from the incidence matrix $\mathcal{H}$. The node embeddings are updated using only the linear aggregation of neighboring nodes' information via the adjacency matrix, represented as:

$$Z^s = \hat{A}^s X W^s \tag{8}$$

where $\hat{A}^s = A^s + I$ and W^s is the trainable weight matrix. To ensure that the TinyGCN captures similar high-order relationships as the HGNN, a contrastive learning approach is applied using the InfoNCE loss:

$$L_{\text{con}} = -\frac{1}{|V|}\sum_{v\in V}\log\left(\frac{\exp\left(Z_v^s \cdot Z_v^t/\tau\right)}{\sum_{v'\in V}\exp\left(Z_{v'}^s \cdot Z_{v'}^t/\tau\right)}\right) \tag{9}$$

where τ is the temperature parameter that scales the similarity scores between embeddings. The total loss for the teacher model combines the supervised and contrastive losses as:

$$L_{\text{teacher}} = L_{\text{bpr}} + \gamma L_{\text{con}} \tag{10}$$

with γ as a hyperparameter balancing the contributions of both losses. This ensures a seamless transfer of the topological structure and high-order information from the HGNN to the TinyGCN.

Additionally, the teacher model generates soft labels for all nodes in the graph, representing the probability distribution over classes for each node. Given the limited availability of human-annotated labels, these soft labels serve as a valuable form of knowledge, transferred to the student model to provide richer supervisory signals. This approach helps the student model effectively learn the underlying data distribution, enabling it to perform well even with a sparse set of ground truth labels.

The student model includes the TinyGCN and a separate MLP. TinyGCN produces embeddings Z^s for each node, which is then fed into the student MLP to predict the target labels. We use both labeled data and soft labels provided by the teacher model to train the student model. For a given node v with node features X_v, the predicted label is:

$$\hat{Y}_v^s = \text{MLP}^s(\text{TinyGCN}(X_v)) \tag{11}$$

The loss function for the student model is:

$$L_{\text{student}} = \frac{1}{|V^L|} \sum_{v \in V^L} (\hat{Y}_v - Y_v)^2 + \lambda \frac{1}{|V|} \sum_{v \in V} \text{KL}(\hat{Y}_v || Y_v^t) \tag{12}$$

where Y_v^t represents the soft label obtained from the teacher model, and KL denotes the Kullback-Leibler divergence, which measures the difference between the predicted probability distribution and the target distribution provided by the teacher. The parameter λ controls the influence of the distillation loss in the overall training objective, balancing the impact of learning from the teacher's knowledge against other learning signals. This approach ensures that the student model effectively assimilates the nuanced class probabilities inferred by the teacher. The algorithm of the proposed method is provided in Algorithm 1 in the Appendix A.

4 EXPERIMENTS

4.1 DATASETS

In our experiments, we utilize eight well-known graph datasets. The Cora dataset, introduced by Sen et al. Sen et al. (2008), and the Citeseer dataset, developed by Giles et al. Giles et al. (1998), have been transformed into hypergraph datasets, namely CC-Cora and CC-Citeseer, by Yadati et al. Yadati et al. (2019). In these two datasets, vertices represent academic papers, and hyperedges connect co-cited papers (CC). Each vertex is labeled according to the topic of its corresponding paper. We include the complete IMDB dataset and its subset IMDBAW from Fu et al. Fu et al. (2019), which features multiple types of hyperedges: user-movie interactions, actor-movie collaborations, and director-movie relationships. While IMDBAW focuses on co-actor and co-director relationships, the complete IMDB encompasses a broader network of 142,129 nodes across movies, users, directors, and actors. Additionally, we incorporate the complete DBLP dataset and its three subsets: DBLP-Paper, DBLP-Term, and DBLP-Conf, as introduced by Sun et al. Sun et al. (2011). The complete DBLP dataset contains 66,543 nodes spanning papers, authors, venues, and terms, with hyperedges formed through various academic relationships. In its subsets, hyperedges are formed based on collaborations (DBLP-Paper), the use of the same term (DBLP-Term), and papers published at the same conference (DBLP-Conf). The vertex labels correspond to the authors' research areas. A summary of the dataset statistics is provided in Table 3 in the Appendix B.

4.2 EVALUATION METHODS

We conducted each experiment five times using different random seeds, reporting both the average performance and standard deviation. Our evaluation is based on three training methods: transductive, inductive, and production Tian et al. (2022); Feng et al. (2024). In the transductive method, the training and test data are used during evaluation, allowing the model to learn from the entire dataset. In contrast, the inductive method trains the model on one dataset and tests it on a completely different, unseen dataset. The production method combines both transductive and inductive predictions to simulate a more realistic deployment scenario. For each dataset, 20% of the data was used for validation, and 10% was used for testing. Accuracy was the primary metric for performance comparison, and the model with the best validation performance was applied to the test set for final evaluation.

4.3 BASELINE METHODS

We evaluate **DistillHGNN** against two different types of approaches. The first category includes graph-based methods, comprising traditional GNN models Scarselli et al. (2008), GCN by Kipf and Welling Kipf & Welling (2016), Multilayer Perceptron (MLP) by Taud et al. Taud & Mas (2018), and knowledge distillation methods. These include GNN-to-MLP models like GLNN by Zhang et al. Zhang et al. (2021) and KRD by Wu et al. Wu et al. (2023), which operate on graph structures. The second category comprises hypergraph-based methods. We utilize the Hypergraph Neural Network (HGNN) by Feng et al. Feng et al. (2019) and the knowledge distillation method HGNN-to-MLP (LightHGNN) by Feng et al. Feng et al. (2024). Accordingly, we generate two versions of the data: for the first type of methods, we use the graph structure, which includes GNN, MLP, and GLNN, while for the second type, we utilize the hypergraph structure for HGNN and LightHGNN. The baseline experiments and our methods are implemented using PyTorch and the DHG library [1]. We evaluate the proposed method for classification based on two key aspects: accuracy and inference speed. Table 1 presents the results based on accuracy across the three training methods.

Table 1: Experimental results on eight hypergraph datasets under production setting.

Dataset	Setting	GNN	GCN	MLP	HGNN	GLNN	KRD	LightHGNN	DistillHGNN
IMDB	Tran.	$46.45_{+2.15}$	$46.92_{+1.65}$	$43.22_{+1.95}$	$51.45_{+1.77}$	$45.88_{+2.33}$	$47.33_{+1.88}$	$50.22_{+1.95}$	$\mathbf{51.88_{+1.66}}$
	Ind.	$47.33_{+2.44}$	$47.67_{+1.72}$	$44.15_{+2.12}$	$52.28_{+1.95}$	$46.85_{+2.55}$	$48.22_{+2.05}$	$51.18_{+2.12}$	$\mathbf{52.33_{+1.77}}$
	Prod.	$46.88_{+2.33}$	$47.15_{+1.88}$	$43.77_{+2.05}$	$51.22_{+1.88}$	$46.12_{+2.44}$	$47.88_{+1.95}$	$50.45_{+2.05}$	$\mathbf{51.92_{+1.66}}$
IMDB-AW	Tran.	$46.26_{+1.36}$	$46.77_{+2.12}$	$42.70_{+1.67}$	$\mathbf{53.36_{+2.25}}$	$45.22_{+2.51}$	$47.15_{+1.88}$	$51.11_{+0.77}$	$52.34_{+1.62}$
	Ind.	$48.28_{+4.43}$	$48.67_{+2.33}$	$43.35_{+3.33}$	$54.12_{+2.74}$	$46.50_{+2.23}$	$49.12_{+2.55}$	$52.27_{+1.14}$	$\mathbf{55.27_{+1.16}}$
	Prod.	$47.33_{+1.82}$	$47.88_{+1.95}$	$43.15_{+1.92}$	$53.31_{+3.01}$	$45.16_{+3.98}$	$48.22_{+2.15}$	$51.84_{+3.51}$	$\mathbf{53.93_{+2.14}}$
CC-Citeseer	Tran.	$53.06_{+0.62}$	$53.88_{+1.62}$	$46.76_{+0.83}$	$\mathbf{62.26_{+1.68}}$	$52.57_{+1.73}$	$54.12_{+1.55}$	$59.65_{+2.12}$	$61.02_{+1.62}$
	Ind.	$55.00_{+1.09}$	$55.22_{+1.88}$	$49.20_{+2.60}$	$\mathbf{62.38_{+2.11}}$	$54.45_{+3.01}$	$55.67_{+2.12}$	$61.36_{+1.27}$	$62.18_{+2.16}$
	Prod.	$53.60_{+0.34}$	$54.05_{+2.01}$	$47.20_{+1.60}$	$61.39_{+3.11}$	$52.08_{+2.55}$	$54.33_{+1.92}$	$60.11_{+1.63}$	$\mathbf{61.88_{+2.14}}$
CC-Cora	Tran.	$52.26_{+3.25}$	$52.88_{+1.95}$	$45.16_{+2.51}$	$\mathbf{65.17_{+1.68}}$	$51.22_{+1.10}$	$53.45_{+2.15}$	$63.65_{+2.12}$	$65.02_{+1.62}$
	Ind.	$54.39_{+2.15}$	$54.67_{+2.05}$	$48.66_{+2.19}$	$\mathbf{66.88_{+2.11}}$	$53.50_{+1.81}$	$55.12_{+1.88}$	$65.76_{+1.27}$	$66.78_{+1.16}$
	Prod.	$54.15_{+3.44}$	$54.55_{+1.92}$	$48.02_{+2.05}$	$65.52_{+2.11}$	$53.19_{+2.75}$	$54.88_{+2.33}$	$64.11_{+1.63}$	$\mathbf{65.68_{+2.14}}$

Dataset	Setting	GNN	GCN	MLP	HGNN	GLNN	KRD	LightHGNN	DistillHGNN
DBLP	Tran.	$75.33_{+2.15}$	$75.92_{+1.88}$	$66.88_{+2.77}$	$\mathbf{83.26_{+1.55}}$	$72.45_{+2.55}$	$76.45_{+1.95}$	$81.45_{+2.88}$	$82.88_{+1.66}$
	Ind.	$76.15_{+2.44}$	$76.67_{+1.95}$	$67.22_{+3.15}$	$84.12_{+1.77}$	$73.12_{+2.88}$	$77.22_{+2.12}$	$82.33_{+2.55}$	$\mathbf{84.45_{+1.88}}$
	Prod.	$75.88_{+2.33}$	$76.15_{+1.92}$	$66.45_{+2.95}$	$83.55_{+1.88}$	$72.88_{+2.66}$	$76.88_{+2.05}$	$81.88_{+2.44}$	$\mathbf{83.77_{+1.75}}$
DBLP-Paper	Prod.	$65.15_{+2.21}$	$65.88_{+1.95}$	$60.47_{+2.44}$	$\mathbf{71.80_{+1.08}}$	$62.42_{+4.02}$	$66.33_{+2.15}$	$69.12_{+3.22}$	$71.22_{+2.55}$
	Tran.	$66.23_{+1.55}$	$66.77_{+2.12}$	$62.38_{+2.45}$	$72.52_{+0.98}$	$63.87_{+3.76}$	$67.12_{+2.33}$	$71.22_{+2.63}$	$\mathbf{72.02_{+1.76}}$
	Ind.	$65.57_{+1.86}$	$66.22_{+2.05}$	$61.50_{+3.07}$	$72.08_{+1.54}$	$63.17_{+3.22}$	$66.88_{+1.92}$	$70.69_{+2.17}$	$\mathbf{71.16_{+1.64}}$
DBLP-Term	Prod.	$66.33_{+2.31}$	$66.92_{+1.88}$	$61.20_{+3.65}$	$\mathbf{72.10_{+0.90}}$	$64.15_{+2.84}$	$67.45_{+2.15}$	$70.16_{+3.29}$	$71.67_{+0.87}$
	Tran.	$67.52_{+3.29}$	$67.88_{+2.15}$	$62.12_{+3.50}$	$73.46_{+1.63}$	$65.24_{+2.72}$	$68.33_{+2.44}$	$71.64_{+1.53}$	$\mathbf{73.79_{+1.32}}$
	Ind.	$66.13_{+4.06}$	$66.77_{+2.05}$	$61.68_{+2.88}$	$\mathbf{73.12_{+1.33}}$	$64.87_{+3.15}$	$67.22_{+2.33}$	$71.51_{+2.17}$	$72.45_{+1.76}$
DBLP-Conf	Prod.	$72.30_{+2.55}$	$72.88_{+1.95}$	$63.53_{+2.77}$	$\mathbf{90.03_{+1.66}}$	$69.18_{+3.11}$	$73.45_{+2.15}$	$88.10_{+3.51}$	$89.27_{+2.17}$
	Tran.	$74.18_{+2.84}$	$74.67_{+2.12}$	$65.12_{+3.44}$	$\mathbf{92.22_{+2.78}}$	$71.45_{+2.23}$	$75.22_{+2.33}$	$90.74_{+4.20}$	$92.11_{+1.84}$
	Ind.	$74.26_{+2.62}$	$74.88_{+2.05}$	$64.22_{+4.07}$	$91.00_{+2.42}$	$71.02_{+2.96}$	$75.33_{+1.92}$	$90.05_{+4.04}$	$\mathbf{91.38_{+3.25}}$

The DistillHGNN model demonstrates substantial advantages in classification tasks by utilizing knowledge distillation to enhance its performance over traditional graph-based and hypergraph-based methods. As shown in Table 1, DistillHGNN consistently achieves either the highest or second-highest accuracy across various datasets and settings, including training (Tran), inductive (Ind), and production (Prod) scenarios. Although DistillHGNN's accuracy is slightly lower than HGNN's top performance, it consistently outperforms LightHGNN and shows a small but noticeable improvement in accuracy. Additionally, DistillHGNN significantly surpasses traditional models such as GNN, GCN, MLP, GLNN and KRD.

[1] https://github.com/iMoonLab/DeepHypergraph

4.4 Balancing Accuracy and Inference Time

Before introducing the results of this section, it is important to note that for all subsequent experiments, we employ the production method for training. Additionally, we use three versions of the DBLP dataset (based on Papers, Terms, and Conferences), running the model on all three variants and taking the average to ensure consistency. This averaged result is referred to as the DBLP dataset in our analysis. In this evaluation phase, we focus on two datasets—IMDB-AW and DBLP—and compare DistillHGNN with other models by examining the trade-off between model accuracy and inference time. This approach allows us to evaluate both the effectiveness and computational efficiency of each model, offering a comprehensive comparison across these dimensions. In real-world applications, an ideal model should maintain high accuracy while minimizing inference time, particularly when computational resources and processing speed are critical. Models with high accuracy but slow inference times, such as GNNs or HGNNs, may not be practical for time-sensitive applications, while faster models like MLPs, which sacrifice accuracy, may fail to meet performance expectations. The strength of knowledge distillation models lies in achieving a balanced trade-off, offering both competitive accuracy and reasonable computational efficiency. Higher accuracy often comes at the expense of longer inference time, but DistillHGNN is designed to balance these factors. The results, illustrated in Figure 2, demonstrate how each model's accuracy compares with its inference time across the datasets.

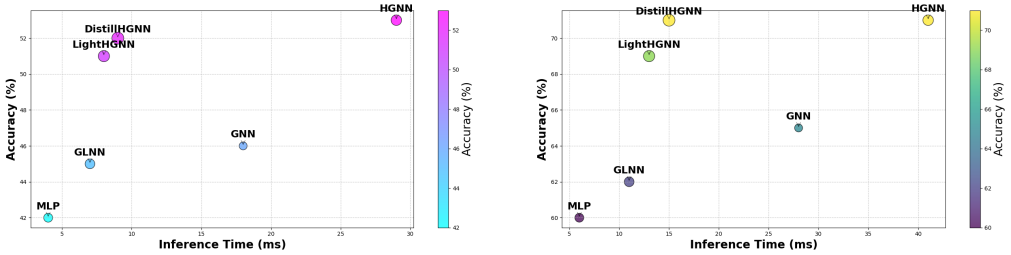

(a) IMDB-AW (Accuracy vs. Inference Time) (b) DBLP (Accuracy vs. Inference Time)

Figure 2: Comparison of Models based on Accuracy and Inference Time

Figure 2 demonstrates that DistillHGNN significantly reduces inference time compared to HGNN, achieving a reduction of approximately 69%. This improvement underscores DistillHGNN's efficiency, as it maintains high accuracy while providing much faster inference. Although MLP offers the quickest inference time at just 4 ms, its accuracy of 0.42 makes it less suitable for high-performance applications. DistillHGNN's inference time is not only significantly faster than HGNN's but also comparable to LightHGNN's, while delivering superior accuracy. This indicates that the knowledge distillation process enhances overall performance without adding substantial computational overhead. Additionally, DistillHGNN outperforms GNN and GLNN in accuracy, making it an effective model for large-scale tasks that require a balance of performance and speed. Overall, DistillHGNN effectively balances high accuracy with computational efficiency, making it an ideal choice for scenarios where both model performance and rapid execution are crucial, such as in real-time systems or large-scale applications.

4.5 Accuracy of the Methods

A key challenge in knowledge distillation is to ensure that the student captures not only direct relationships between nodes but also crucial high-order relations. In this process, we focus on two relationship types within the student model: direct (neighboring) relations and high-order relations. The teacher model, leveraging a hypergraph structure, excels at capturing high-order relationships but often suffers from high inference times due to the complexity of hyperedges.

Previous research, such as Tian et al. (2022); Wu et al. (2023); Feng et al. (2024), has utilized soft labels to facilitate knowledge transfer. However, while soft labels approximate the teacher's behavior, they alone cannot fully convey the high-order structural knowledge captured by the hypergraph. To overcome this limitation, we propose a combined approach that utilizes both soft labels and structural knowledge from the Hypergraph Neural Network (HGNN) as the teacher model. To implement this combined distillation, we employ contrastive learning within the TinyGCN framework.

The student model receives two types of inputs: one based on the simpler TinyGCN architecture and the other derived from high-order embeddings generated by the HGNN teacher model. To evaluate the effectiveness of DistillHGNN, we propose the High-Order Preservation Score (H_{pres}), which quantifies how well the student model retains the complex, high-order relationships transferred from the teacher model. DistillHGNN addresses this challenge by incorporating both soft labels and high-order relation embeddings through contrastive learning. The High-Order Preservation Score is computed as follows:

$$H_{\text{pres}} = \frac{1}{|V|} \sum_{v \in V} \frac{1}{K} \sum_{u \in N_K(v)} \text{Sim}(\mathbf{x}_u^{\text{teacher}}, \mathbf{x}_u^{\text{student}}) \tag{13}$$

Here, $|V|$ is the total number of nodes, $N_K(v)$ is the set of K-nearest neighbors of node v, and $\mathbf{x}_u^{\text{teacher}}$ and $\mathbf{x}_u^{\text{student}}$ are the embeddings generated by the teacher and student models, respectively. The similarity measure Sim can be based on cosine similarity or Euclidean distance, depending on the experimental setup. This score evaluates the extent to which the student model replicates the high-order structural information encoded in the teacher model, focusing on the similarity between the embeddings of neighboring nodes in both models. The results indicate in Table 2 as follows: The results demonstrate a clear progression in the High-Order Relation Preservation Score (H_{pres})

Table 2: Comparison of Knowledge Distillation Methods Based on Preservation Scores Across Datasets

Method	**CC-Cora**	**CC-Citeseer**	**IMDB-AW**	**DBLP**	*Mean*
GLNN Tian et al. (2022)	0.54	0.58	0.51	0.67	**0.575**
KRD Wu et al. (2023)	0.56	0.62	0.54	0.71	**0.6075**
LightHGNN Feng et al. (2024)	0.72	0.78	0.74	0.83	**0.7675**
DistillHGNN	0.78	0.84	0.81	0.88	**0.8275**

across the evaluated methods, with DistillHGNN achieving the highest mean score of 0.8275. This indicates that methods integrating greater structural knowledge are significantly more effective at preserving high-order relationships.

4.6 Inference Time

MLPs offer faster execution times and lower memory usage but typically result in reduced accuracy. In contrast, HGNNs deliver superior performance, though at the cost of slower inference times and higher memory consumption. DistillHGNN successfully bridges this gap by achieving a balanced trade-off between memory usage and accuracy. As illustrated in Figure 2, DistillHGNN maintains competitive inference times and reduces memory consumption through its lightweight student model design without sacrificing accuracy. By utilizing heterogeneous graphs, such as those derived from the IMDB and DBLP datasets Fan et al. (2021), the model benefits from the rich, multi-relational structures present in the data. These datasets include complex relationships where nodes—such as movies or academic papers—interact with various entities (e.g., users, directors, authors), forming hyperedges that capture higher-order connections. Detailed statistics of the datasets and the results from this evaluation are presented in Tables 4 and 5, respectively, in Appendix C.

4.7 Ablation Study

In this section, we present findings that evaluate the effectiveness of different knowledge transfer methods employed in the DistillHGNN framework. The proposed model is assessed using three distinct approaches: (1) soft labels alone, (2) structural knowledge alone, and (3) a combination of both (DistillHGNN). The results are illustrated in Figure 3, which includes calculations of both accuracy and inference time for each method. The findings are presented in Figure 3 as follows: The accuracy scores reveal a significant improvement when using the combined approach of DistillHGNN, which leverages both soft labels and structural knowledge, compared to using either method individually. Across all datasets, the combined method consistently outperforms the individual approaches, with accuracy improvements ranging from 3% to 10%. These findings underscore the advantages of utilizing both soft labels and structural knowledge within the DistillHGNN framework, demonstrating a favorable trade-off between speed and accuracy.

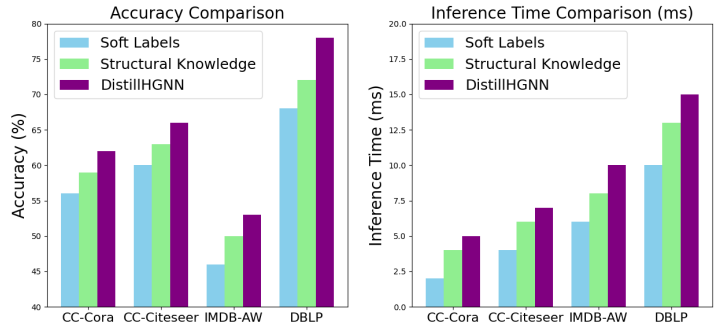

Figure 3: The proposed model is evaluated using three different knowledge transfer methods: (1) soft labels alone, (2) structural knowledge alone, and (3) a combination of both (DistillHGNN). The evaluation includes calculating both accuracy and inference time for each method.

In DistillHGNN, knowledge transfer occurs through both structural knowledge and soft labels from the teacher model to the student model. When CL is incorporated, the model achieves a more refined alignment of node embeddings, enabling the student to effectively capture intricate high-order relationships. The results comparing models with and without CL are presented in Figure 4 as follows: The accuracy comparison between the models with and without contrastive learning across datasets

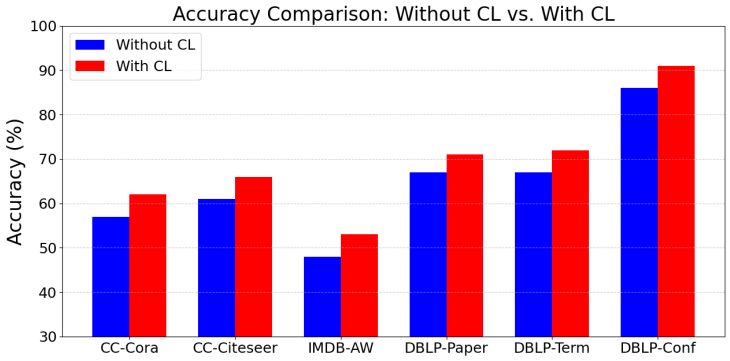

Figure 4: The proposed model is evaluated based on the absence of contrastive learning (lack of CL) and with contrastive learning (DistillHGNN), focusing on accuracy across four datasets.

clearly shows performance improvements when using CL. These results indicate that incorporating both structural knowledge and contrastive learning in DistillHGNN enhances generalization and performance, particularly in more complex datasets like DBLP. Despite slightly slower inference times, the accuracy gains justify the use of DistillHGNN for achieving more accurate predictions.

To further evaluate the performance of DistillHGNN, we examine the impact of increasing the number of layers in the proposed model on both accuracy and inference time. This analysis helps determine the influence of model depth on the quality of predictions and computational efficiency across HGNN, Teacher MLP, TinyGCN, and Distill MLP. The results of this evaluation are presented in Appendix D.

In the context of the proposed DistillHGNN method, several hyperparameters play key roles in controlling the trade-offs between different components, the learning process, and overall performance. Table 6 shows the results of the evaluation of the DistillHGNN framework based on different configurations of hyperparameters and their corresponding accuracy metrics in Appendix E.

In this experiment, we evaluate the performance of DistillHGNN across six hypergraph datasets under different training sizes. The goal is to observe how varying the proportion of training data affects the model's accuracy. We compare the DistillHGNN model with several baselines: GNNs, MLP, GLNN, HGNN, and LightHGNN. The results are presented in Table 7 in Appendix F.

To thoroughly assess the performance of DistillHGNN, we conducted an ablation study focusing on the impact of different training durations, specifically varying the number of training epochs. This evaluation aims to determine how the duration of training influences the model's accuracy and generalization capability across different datasets. Each model was trained using the same dataset and hyperparameter settings to ensure a fair comparison. The results of this study are shown in Figure 5, which presents the accuracy achieved by DistillHGNN for each training epoch setting.

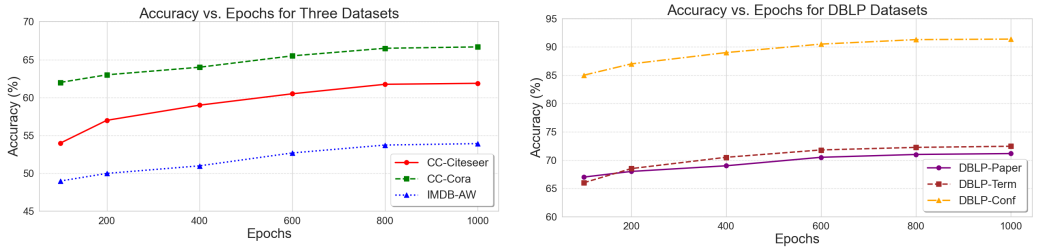

(a) CC-Citeseer, CC-Cora, and IMDB-AW Datasets

(b) DBLP Datasets

Figure 5: Sensitivity analysis of training epoch settings ranging from 100 to 1000. This analysis aims to evaluate how varying the number of training epochs influences model performance, providing insights into the optimal training duration for achieving the best accuracy.

The experimental results indicate that as the number of epochs increases, model accuracy generally improves, though at varying rates depending on the dataset. This result indicates that the datasets contains rich features that the model can leverage effectively, benefiting substantially from additional training epochs.

4.8 Visual Analysis of Knowledge Transfer

We conducted a comprehensive visual analysis of DistillHGNN's performance using multiple visualization techniques to evaluate the effectiveness of knowledge transfer between teacher and student models. The results of this evaluation are presented in Appendix G.

5 Conclusion

In this paper, we address two key challenges in knowledge distillation for graph-based models: (1) effectively transferring high-order relationships between nodes, and (2) overcoming the limitations of using soft labels as the sole medium for transferring knowledge from the teacher model to the student model. To address the first challenge, we leveraged a hypergraph structure within the teacher model, allowing for the capture and transfer of high-order relationships that go beyond direct node connections. For the second challenge, we employed a CL framework in combination with soft labels to enhance the knowledge transfer process. The contrastive learning mechanism ensures that the embeddings generated by the student model align with those of the teacher model, thereby preserving the high-order relational knowledge encoded in the HGNN. The experimental results demonstrate that the proposed approach achieves superior accuracy compared to traditional knowledge distillation methods. Specifically, the use of hypergraph-based embeddings and the integration of soft label distillation with structural knowledge led to better performance in terms of both classification accuracy and the preservation of high-order node relations. Moreover, our method strikes a desirable balance between inference speed and memory efficiency. Although TinyGCN significantly reduces computational complexity, its performance remains comparable to that of the more complex HGNN model. Overall, this approach opens up new possibilities for lightweight models that retain the expressiveness of more complex networks while ensuring faster inference, making it suitable for real-world applications where computational resources are limited.

References

Alessia Antelmi, Gennaro Cordasco, Mirko Polato, Vittorio Scarano, Carmine Spagnuolo, and Dingqi Yang. A survey on hypergraph representation learning. *ACM Computing Surveys*, 56

(1):1–38, 2023.

Song Bai, Feihu Zhang, and Philip HS Torr. Hypergraph convolution and hypergraph attention. *Pattern Recognition*, 110:107637, 2021.

Yihe Dong, Will Sawin, and Yoshua Bengio. Hnhn: Hypergraph networks with hyperedge neurons. *arXiv preprint arXiv:2006.12278*, 2020.

Haoyi Fan, Fengbin Zhang, Yuxuan Wei, Zuoyong Li, Changqing Zou, Yue Gao, and Qionghai Dai. Heterogeneous hypergraph variational autoencoder for link prediction. *IEEE transactions on pattern analysis and machine intelligence*, 44:4125–4138, 2021.

Yifan Feng, Haoxuan You, Zizhao Zhang, Rongrong Ji, and Yue Gao. Hypergraph neural networks. In *Proceedings of the AAAI conference on artificial intelligence*, volume 33, pp. 3558–3565, 2019.

Yifan Feng, Yihe Luo, Shihui Ying, and Yue Gao. Lighthgnn: Distilling hypergraph neural networks into mlps for 100x faster inference. In *The Twelfth International Conference on Learning Representations*, 2024.

Sichao Fu, Weifeng Liu, Yicong Zhou, and Liqiang Nie. Hplapgcn: Hypergraph p-laplacian graph convolutional networks. *Neurocomputing*, 362:166–174, 2019.

Yue Gao, Yifan Feng, Shuyi Ji, and Rongrong Ji. Hgnn+: General hypergraph neural networks. *IEEE Transactions on Pattern Analysis and Machine Intelligence*, 45(3):3181–3199, 2022.

C Lee Giles, Kurt D Bollacker, and Steve Lawrence. Citeseer: An automatic citation indexing system. In *Proceedings of the third ACM conference on Digital libraries*, pp. 89–98, 1998.

Malik Khizar Hayat, Shan Xue, Jia Wu, and Jian Yang. Heterogeneous hypergraph embedding for node classification in dynamic networks. *IEEE Transactions on Artificial Intelligence*, 2024.

Jianwen Jiang, Yuxuan Wei, Yifan Feng, Jingxuan Cao, and Yue Gao. Dynamic hypergraph neural networks. In *IJCAI*, pp. 2635–2641, 2019.

Thomas N Kipf and Max Welling. Semi-supervised classification with graph convolutional networks. *arXiv preprint arXiv:1609.02907*, 2016.

Jing Liu, Tongya Zheng, and Qinfen Hao. Hire: Distilling high-order relational knowledge from heterogeneous graph neural networks. *Neurocomputing*, 507:67–83, 2022.

Nicolò Ruggeri, Alessandro Lonardi, and Caterina De Bacco. Message-passing on hypergraphs: detectability, phase transitions and higher-order information. *Journal of Statistical Mechanics: Theory and Experiment*, 2024(4):043403, 2024.

Franco Scarselli, Marco Gori, Ah Chung Tsoi, Markus Hagenbuchner, and Gabriele Monfardini. The graph neural network model. *IEEE transactions on neural networks*, 20(1):61–80, 2008.

Prithviraj Sen, Galileo Namata, Mustafa Bilgic, Lise Getoor, Brian Galligher, and Tina Eliassi-Rad. Collective classification in network data. *AI magazine*, 29(3):93–93, 2008.

Yizhou Sun, Jiawei Han, Xifeng Yan, Philip S Yu, and Tianyi Wu. Pathsim: Meta path-based top-k similarity search in heterogeneous information networks. *Proceedings of the VLDB Endowment*, 4(11):992–1003, 2011.

Hind Taud and Jean-Franccois Mas. Multilayer perceptron (mlp). *Geomatic approaches for modeling land change scenarios*, pp. 451–455, 2018.

Yijun Tian, Chuxu Zhang, Zhichun Guo, Xiangliang Zhang, and Nitesh Chawla. Learning mlps on graphs: A unified view of effectiveness, robustness, and efficiency. In *The Eleventh International Conference on Learning Representations*, 2022.

Hanrui Wu, Yuguang Yan, and Michael Kwok-Po Ng. Hypergraph collaborative network on vertices and hyperedges. *IEEE Transactions on Pattern Analysis and Machine Intelligence*, 45(3):3245–3258, 2022.

Lirong Wu, Haitao Lin, Yufei Huang, and Stan Z Li. Quantifying the knowledge in gnns for reliable distillation into mlps. In *International Conference on Machine Learning*, pp. 37571–37581. PMLR, 2023.

Naganand Yadati, Madhav Nimishakavi, Prateek Yadav, Vikram Nitin, Anand Louis, and Partha Talukdar. Hypergcn: A new method for training graph convolutional networks on hypergraphs. *Advances in neural information processing systems*, 32, 2019.

Jielong Yan, Yifan Feng, Shihui Ying, and Yue Gao. Hypergraph dynamic system. In *The Twelfth International Conference on Learning Representations*, 2024.

Cheng Yang, Jiawei Liu, and Chuan Shi. Extract the knowledge of graph neural networks and go beyond it: An effective knowledge distillation framework. In *Proceedings of the web conference 2021*, pp. 1227–1237, 2021.

Nan Yin, Fuli Feng, Zhigang Luo, Xiang Zhang, Wenjie Wang, Xiao Luo, Chong Chen, and Xian-Sheng Hua. Dynamic hypergraph convolutional network. In *2022 IEEE 38th International Conference on Data Engineering (ICDE)*, pp. 1621–1634. IEEE, 2022.

Beibei Yu, Cheng Xie, Hongming Cai, Haoran Duan, and Peng Tang. Meta-path and hypergraph fused distillation framework for heterogeneous information networks embedding. *Information Sciences*, 667:120453, 2024.

Li ZENG, Jing-Ru YANG, Gang HUANG, Xiang YING, and Tiao-Ran LUO. Survey on hypergraph application methods: Research problem, progress, and challenges. *Journal of Computer Applications*, pp. 0, 2024.

Shichang Zhang, Yozen Liu, Yizhou Sun, and Neil Shah. Graph-less neural networks: Teaching old mlps new tricks via distillation. *arXiv preprint arXiv:2110.08727*, 2021.

A ALGORITHM

The proposed DistillHGNN framework is a knowledge distillation approach that leverages the power of a Hypergraph Neural Network (HGNN) as the teacher model and a lightweight TinyGCN (Graph Convolutional Network) as the student model. The goal of this framework is to transfer knowledge from the HGNN, which captures high-order relations among nodes through hyperedges, to the TinyGCN, which is designed for direct and low-complexity node aggregation. By distilling the rich information from the teacher model into the simpler student model, the system ensures efficient learning while maintaining competitive performance in tasks such as node classification. The distillation process includes the generation of soft labels from the teacher model, which are used as targets for the student model in conjunction with the true labels. Additionally, a contrastive loss function ensures that the embeddings produced by the student model align with the high-order relational embeddings learned by the teacher, reinforcing the transfer of meaningful information. The combination of BPR loss, contrastive loss, and KL divergence enables a robust learning process for the student model. The overall procedure of the proposed DistillHGNN method is outlined in Algorithm 1.

B DATASETS

In this work, we evaluate the performance of the proposed DistillHGNN framework on several widely used benchmark datasets. These datasets come from various domains, including citation networks, movie databases, and bibliographic datasets, providing a diverse range of graph structures and node features. The IMDB dataset represents a comprehensive heterogeneous network from the Internet Movie Database, containing 142,129 nodes across four different types: movies (40,635 nodes), users (2,113 nodes), directors (4,060 nodes), and actors (95,321 nodes). The heterogeneous nature is reflected in its three types of relationships: user-movie interactions (1,216,358 edges), director-movie connections (15,732 edges), and actor-movie collaborations (364,058 edges). With a high average degree of 22.46, this dataset exhibits very dense connectivity patterns, making it particularly challenging for graph learning tasks.

Algorithm 1 DistillHGNN Framework with Knowledge Distillation

Input: Hypergraph $G = \{V, E\}$, features X, incidence matrix $\mathcal{H}$, labeled data $D_L = \{V_L, Y_L\}$, number of epochs E, parameters τ, γ, λ
Output: Student model parameters

Initialize: Parameters for HGNN ($\Theta^{(l)}$), Teacher MLP (Θ^t), Student TinyGCN (W^s), and Student MLP (Θ^s)
Step 1: Compute Laplacian and Adjusted Adjacency
$L \leftarrow D_v^{-1/2}\mathcal{H}WD_e^{-1}\mathcal{H}^\top D_v^{-1/2}$
$\hat{A}^s \leftarrow A^s + I$
Step 2: Pre-train the Teacher Model
for epoch $= 1$ to E **do**
  Compute HGNN embeddings: $Z^t \leftarrow H^L$, where

$$H^{(l+1)} = \sigma(LH^{(l)}\Theta^{(l)})$$

  Generate teacher predictions: $Y^t \leftarrow \text{MLP}^t(Z^t)$
  Compute TinyGCN embeddings: $Z^s \leftarrow \hat{A}^s X W^s$
  Compute teacher loss:

$$L_{\text{teacher}} \leftarrow \frac{1}{|V_L|}\sum_{v\in V_L}(Y_v - Y_v^t)^2 - \gamma\frac{1}{|V|}\sum_{v\in V}\log\frac{\exp(Z_v^s \cdot Z_v^t/\tau)}{\sum_{v'}\exp(Z_{v'}^s \cdot Z_{v'}^t/\tau)}$$

  Update teacher parameters Θ^t and freeze them
end for
Step 3: Train the Student Model
for epoch $= 1$ to E **do**
  Generate teacher outputs: Z^t, Y^t (using frozen teacher model)
  Compute student outputs:

$$Z^s \leftarrow \hat{A}^s X W^s, \quad \hat{Y}_v^s \leftarrow \text{MLP}^s(Z^s)$$

  Compute student loss:

$$L_{\text{student}} \leftarrow \frac{1}{|V_L|}\sum_{v\in V_L}(\hat{Y}_v^s - Y_v)^2 + \lambda\frac{1}{|V|}\sum_{v\in V}\text{KL}(\hat{Y}_v^s \| Y_v^t)$$

  Update student parameters $\{W^s, \Theta^s\}$
end for
Return: Student model parameters

The DBLP dataset is a heterogeneous bibliographic network comprising 66,543 nodes of four types: papers (43,128 nodes), authors (14,475 nodes), venues (20 nodes), and terms (8,920 nodes). The heterogeneity is manifested in its diverse edge types: author-paper collaborations (58,592 edges), venue-paper publications (20,770 edges), and term-paper associations (195,462 edges). With an average degree of 8.26, it presents a dense, interconnected structure while maintaining clear hierarchical relationships among different node types. CC-Citeseer and CC-Cora are standard citation network datasets where nodes represent research papers, and edges represent citation links between papers. These datasets are characterized as homogeneous due to their uniform node and edge types. Each paper (node) is represented by a bag-of-words feature vector, and the goal is to classify papers into different research topics. Their relatively low average degrees (3.2 and 3.8 respectively) indicate sparse connectivity patterns. IMDB-AW is a subset of the complete IMDB dataset that focuses on actor collaborations and relationships within the movie industry. Nodes represent actors, and edges connect actors who have appeared in the same movie. Despite being smaller than the complete IMDB dataset, it maintains its heterogeneous characteristics with an average degree of 8.4, indicating dense connectivity patterns.

DBLP-paper, DBLP-term, and DBLP-Conf are subsets of the complete DBLP bibliographic dataset, each highlighting different aspects of the academic network. These subsets maintain the heterogeneous nature of the complete dataset but with varying connectivity patterns:

1. DBLP-paper exhibits moderate connectivity (degree 5.2) focusing on paper-centric relationships.
2. DBLP-term shows higher connectivity (degree 7.1) emphasizing term-paper associations.
3. DBLP-Conf demonstrates sparse but hierarchical structure (degree 284.2) concentrating on conference-paper relationships.

The summary of the dataset statistics, including the number of nodes, edges (or hyperedges), features, and classes, is provided in Table 3. This diverse collection of datasets, ranging from sparse homogeneous to very dense heterogeneous networks, allows for comprehensive evaluation of hypergraph-based methods across different network structures and application domains.

Table 3: Information on Hypergraph Datasets

Dataset	**Statistics**				**Characteristics**
	#Nodes	#Edges	#Feat	#Class	
DBLP	66,543	274,824	334	4	Dense, heterogeneous (deg=8.26)
IMDB	142,129	1,596,148	3,066	3	Very dense, heterogeneous (deg=22.46)
CC-Citeseer	3,312	1,004	3,703	6	Sparse, homogeneous (deg=3.2)
CC-Cora	2,708	1,483	1,433	7	Mod. sparse, homogeneous (deg=3.8)
IMDB-AW	5,355	6,811	3,066	3	Dense, heterogeneous (deg=8.4)
DBLP-paper	14,376	14,475	334	4	Moderate, heterogeneous (deg=5.2)
DBLP-term	14,376	13,789	334	4	High connect., heterogeneous (deg=7.1)
DBLP-Conf	14,376	1,612	334	4	Sparse, hierarchical (deg=284.2)

C Comparison of DistillHGNN and HGNN Model Based on Inference Time

In this evaluation phase, we assess the inference time of the DistillHGNN model using two heterogeneous datasets: IMDB and DBLP. These datasets are particularly challenging due to their diverse node types and complex relationships, making them ideal for evaluating both the effectiveness and computational performance of our model. The IMDB dataset comprises user, movie, director, and actor nodes, interconnected through various hyperedges, including user-movie, director-movie, and actor-movie relationships. This structure exemplifies a typical heterogeneous network where multiple node types and interactions are represented. Similarly, the DBLP dataset includes paper, author, venue, and term nodes, connected through their respective relationships (author-paper, venue-paper, and term-paper), representing another common structure found in academic collaboration networks.

Table 4 summarizes the key statistics of these datasets, including the number of nodes, types of nodes, and hyperedges. The complexity and scale of these datasets pose significant challenges in terms of inference time, making them ideal for evaluating DistillHGNN's ability to balance accuracy and computational efficiency.

Given the intricacies of these datasets, it is crucial to evaluate the inference time of DistillHGNN in comparison to the original HGNN model. This section aims to assess the inference performance of DistillHGNN on both IMDB and DBLP graphs, contrasting it with the performance of the standard HGNN model. The results, which include a comparative analysis of the inference times, are summarized in Table 5. These findings illustrate the efficiency of DistillHGNN in reducing inference time while maintaining competitive performance.

These results highlight the scalability and computational efficiency of DistillHGNN, especially when managing large-scale graphs. For example, with 40,635 nodes in the IMDB dataset, DistillHGNN demonstrates an impressive speed improvement, being almost 79 times faster than the HGNN model. Similarly, for the DBLP dataset with 43,128 nodes, DistillHGNN is nearly 82 times faster. The substantial speedup, particularly at larger node levels, underscores the practical advantages of Distill-

Table 4: Statistics of the Datasets

Dataset	Nodes	Count of Nodes	Hyperedges	Count of Edges
IMDB	Movie	40,635		
	User	2,113	User-Movie	1,216,358
	Director	4,060	Director-Movie	15,732
	Actor	95,321	Actor-Movie	364,058
	Total	142,129		1,596,148
DBLP	Paper	43,128		
	Author	14,475	Author-Paper	58,592
	Venue	20	Venue-Paper	20,770
	Term	8,920	Term-Paper	195,462
	Total	66,543		274,824

Table 5: Comparison of Inference Time (ms) between DistillHGNN and HGNN for IMDB and DBLP Datasets at Different Node Levels.

Dataset	Hyperedge Count	HGNN	DistillHGNN	Improvement (%)
IMDB	10,000	8.12	0.67	12.12
	20,000	37.35	1.13	33.05
	30,000	84.70	1.68	50.42
	40,635	175.56	2.23	78.70
DBLP	10,000	9.47	0.72	13.15
	20,000	42.15	0.98	43.01
	30,000	75.33	1.51	49.88
	43,128	168.84	2.06	81.97

HGNN in applications that require rapid inference on complex, multi-relational data. Furthermore, the consistently higher times-faster ratios across both datasets accentuate DistillHGNN's effectiveness in minimizing computational overhead compared to the HGNN model. Overall, the analysis illustrates that DistillHGNN not only maintains competitive performance but also significantly enhances inference speed, making it a compelling choice for real-world applications that demand efficiency without sacrificing accuracy. This capability is particularly valuable in scenarios where the processing of vast amounts of data is required, such as recommendation systems and social network analyses.

D Evaluation of DistillHGNN Based on the Depth of Layers Configuration

To further assess the performance of DistillHGNN, we evaluate the impact of increasing the number of layers in various sections of the proposed model. This includes the HGNN and Teacher MLP in the Teacher section, as well as TinyGCN and Distill MLP in the Student section, with a focus on accuracy and inference time. The selected layers for the proposed method include three layers for both HGNN and Teacher MLP, a single layer for TinyGCN, and two layers for Distill MLP. In this section, we experiment with each model by testing different configurations with multiple layers (specifically, 2, 3, 4, and 5 layers) and comparing the results based on accuracy and inference time. Our experiments are conducted on the IMDB-AW dataset, and the results are illustrated in Figure 6 as follows:

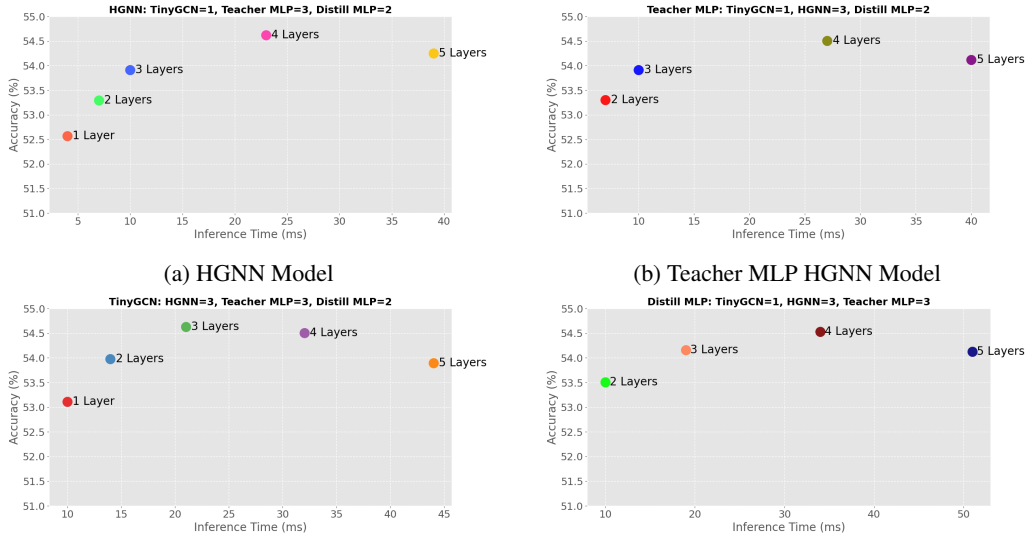

(a) HGNN Model

(b) Teacher MLP HGNN Model

(c) TinyGCN Model

(d) Distill MLP Model

Figure 6: Evaluation of the Proposed Method Based on the Depth of Layers Configuration for HGNN, Teacher MLP, TinyGCN, and Distilled MLP using the IMDB-AW Dataset

In evaluating the performance of DistillHGNN, as indicated in Figure 6, we analyzed the impact of increasing the number of layers across different sections of the proposed model, including the HGNN and Teacher MLP in the Teacher section, as well as TinyGCN and Distill MLP in the Student section. The analysis focused on accuracy and inference time, based on the results obtained. The selected layers for the proposed method include three layers for both HGNN and Teacher MLP, a single layer for TinyGCN, and two layers for Distill MLP. This selection is driven by the need to balance model complexity with computational efficiency while ensuring optimal performance. The HGNN model demonstrates a consistent upward trend in accuracy as the number of layers increases, starting from 52.37% with 1 layer and reaching 54.15% with 5 layers. However, the decision to limit the depth of the HGNN to three layers is based on observed diminishing returns in accuracy beyond this point, as indicated by the marginal improvement from 54.12% at 4 layers to 54.15% at 5 layers.

This suggests that three layers are sufficient to capture the essential relationships in the data while minimizing inference time, which escalates from 4 ms to 39 ms with increased depth.

Similarly, the Teacher MLP model shows a relatively stable accuracy range, peaking at 54.11% with 4 layers before slightly dropping to 54.02% at 5 layers. Selecting three layers for the Teacher MLP balances complexity and performance, as it allows the model to learn effectively without succumbing to overfitting or unnecessary computational overhead, particularly since inference time increases significantly from 7 ms at 2 layers to 40 ms at 5 layers. For TinyGCN, which reached its highest accuracy of 54.03% at 3 layers before slightly declining to 53.90% at 5 layers, a single layer was selected to maintain efficiency in inference time while still leveraging the strengths of graph convolution. The increase in accuracy from 53.91% with a single layer to 54.03% at 3 layers is marginal, indicating that a more straightforward architecture is sufficient to capture the essential features of the dataset without incurring excessive computational costs, as inference time ranges from 10 ms to 44 ms with increasing depth. In the case of the Distill MLP model, selecting two layers allows for enhanced performance, reaching an accuracy of 54.33% at 4 layers while still being computationally feasible. The results indicate that two layers strike an effective balance between learning capacity and inference efficiency, given that the inference time increases significantly from 10 ms to 51 ms as layers are added.

In summary, the proposed model's architecture is optimized through careful selection of layer depths tailored to each component's strengths and limitations. Three layers for both HGNN and Teacher MLP allow for capturing complex relationships while avoiding overfitting and excessive inference time. A single layer for TinyGCN maximizes efficiency, while two layers for Distill MLP ensure sufficient capacity for accurate predictions without significant computational overhead. This thoughtful arrangement provides a robust framework for model performance, emphasizing the critical balance between accuracy and operational efficiency. These findings are visually represented in Figure 6, providing further insights into how model architecture affects performance.

E SENSITIVELY HYPERPARAMETERS

In the context of the proposed DistillHGNN method, several hyperparameters play key roles in controlling the trade-offs between different components, the learning process, and overall performance. Below is a brief explanation of the most important hyperparameters:

1. **Temperature for contrastive learning (τ)**: This temperature parameter scales the similarity scores between student and teacher embeddings. A lower value of τ results in sharper, more distinct similarity scores, while a higher value leads to softer comparisons.
2. **Contrastive loss weight** (γ): This hyperparameter balances the importance of the contrastive loss relative to the BPR loss in the teacher model. A higher value of γ increases the influence of contrastive learning.
3. **Distillation loss weight** (λ): This hyperparameter controls the contribution of the distillation loss in the student model. A higher value emphasizes learning from the teacher model's soft labels, while a lower value focuses more on the ground truth labels.
4. **Learning Rate *lr***: The rate at which the model updates its parameters during training. A lower learning rate ensures more gradual convergence but may slow down the training process.
5. **Embedding Dimension**: This determines the size of the embedding vectors generated by both the teacher and student models. Higher dimensions can potentially capture more information, but at the cost of increased computation.

Table 6 shows the results of evaluating the DistillHGNN framework based on different configurations of hyperparameters and their corresponding accuracy metrics.

The evaluation of the DistillHGNN framework, based on various hyperparameter configurations, reveals interesting patterns in model performance. The temperature for contrastive learning (τ) plays a crucial role in the accuracy, with an optimal value of 0.5 yielding the highest accuracy of 78.33%. Similarly, the contrastive loss weight (γ) shows an increase in performance as its value rises, peaking at 0.4. Distillation loss weight (λ) has a more consistent influence, with the best result

Table 6: Hyperparameter Configurations for DistillHGNN on the DBLP

Config	τ	γ	λ	**Embed Dim**	**Learning Rate (lr)**	**Accuracy (%)**
1	0.1	-	-	-	-	76.20
2	0.2	-	-	-	-	76.85
3	0.3	-	-	-	-	77.79
4	0.4	-	-	-	-	78.05
5	0.5	-	-	-	-	**78.33**
6	0.6	-	-	-	-	78.02
7	0.7	-	-	-	-	77.64
Config	-	γ	-	-	-	**Accuracy (%)**
1	-	0.1	-	-	-	77.55
2	-	0.2	-	-	-	77.83
3	-	0.3	-	-	-	78.11
4	-	0.4	-	-	-	**78.33**
5	-	0.5	-	-	-	77.80
6	-	0.6	-	-	-	77.61
Config	-	-	λ	-	-	**Accuracy (%)**
1	-	-	0.1	-	-	77.87
2	-	-	0.2	-	-	**78.33**
3	-	-	0.3	-	-	78.30
4	-	-	0.4	-	-	78.21
Config	-	-	-	**Embed Dim**	-	**Accuracy (%)**
1	-	-	-	32	-	74.48
2	-	-	-	64	-	77.75
3	-	-	-	128	-	**78.33**
4	-	-	-	256	-	77.17
5	-	-	-	512	-	76.59
Config	-	-	-	-	lr	**Accuracy (%)**
1	-	-	-	-	0.1	76.25
2	-	-	-	-	0.5	75.15
3	-	-	-	-	0.001	**78.33**
4	-	-	-	-	0.005	77.23
5	-	-	-	-	0.0001	77.61
Best Hyperparameters Combinations						
1	**0.5**	**0.4**	**0.2**	**128**	**0.001**	**78.33**

observed at 0.2. When analyzing embedding dimensions, 128 emerges as the most effective, balancing representation richness with computational cost. Finally, the learning rate (lr) of 0.001 proves optimal, enabling the model to converge effectively. The best-performing configuration, combining these hyperparameters, demonstrates the importance of fine-tuning to achieve maximal accuracy. This suggests that the interaction between the temperature, loss weights, embedding dimension, and learning rate is crucial for optimizing the DistillHGNN framework.

F Training Size Settings

In this section, we evaluate the performance of DistillHGNN under varying training size settings across six hypergraph datasets. The primary objective is to understand how increasing the amount of training data influences the model's accuracy compared to several baseline models: GNNs, MLP, GLNN, HGNN, and LightHGNN. By setting the training sizes to 20%, 40%, 60%, and 80%, we

aim to observe the progression of each model's performance as more data becomes available. This analysis helps us assess the scalability and effectiveness of each method as the volume of training data increases. The table below presents the results of our experiments, where we report the accuracy for each model across different datasets and training sizes.

Table 7: Experimental results on six hypergraph datasets under various training settings.

Dataset	Train size	GNNs	MLP	GLNN	HGNN	LightHGNN	DistillHGNN
CC-Citeseer	20%	46.40	40.29	44.27	**56.42**	54.76	55.18
	40%	49.66	43.18	48.17	**58.77**	58.11	58.42
	60%	52.14	45.65	50.87	**61.13**	60.19	60.34
	80%	55.20	48.34	53.77	62.23	62.05	**62.44**
CC-Cora	20%	48.32	41.74	46.92	**60.17**	59.05	58.34
	40%	50.61	44.22	49.19	**62.54**	61.58	61.56
	60%	52.06	46.16	51.50	64.69	64.01	**64.83**
	80%	55.50	48.58	54.79	66.04	65.28	**66.81**
IMDB-AW	20%	39.27	35.76	40.77	**48.50**	47.69	47.16
	40%	43.82	39.27	42.66	**49.42**	49.08	49.15
	60%	46.42	41.29	44.33	52.08	51.65	**52.26**
	80%	49.65	45.25	47.44	55.03	53.86	**55.35**
DBLP	20%	61.53	55.80	59.47	**70.41**	69.02	69.44
	40%	65.21	57.17	63.43	**74.73**	73.73	74.65
	60%	68.12	61.40	67.00	**78.63**	77.55	78.16
	80%	70.14	64.09	69.04	80.42	79.35	**80.61**

The experimental results demonstrate that as the training size increases from 20% to 80%, all models generally show improved performance, with DistillHGNN consistently outperforming the baseline methods across all datasets. Notably, in the DBLP dataset, DistillHGNN achieves the highest accuracy at 80% training size with a value of 80.61%. Similarly, in CC-Citeseer and CC-Cora, the performance gap between DistillHGNN and the other models widens as the training size increases. This suggests that DistillHGNN benefits more from additional training data compared to the other models, particularly on larger datasets. While HGNN and LightHGNN also perform well, DistillHGNN's knowledge distillation, which combines structural knowledge with soft labels based on high-order relations, contributes to its superior performance, making it the most effective model across various training settings.

G Visual Analysis of Knowledge Transfer

To comprehensively assess the effectiveness of knowledge transfer in DistillHGNN, we employ visual analysis as a key evaluation tool. Visualization offers intuitive insights into how well the student model learns from the teacher model, complementing numerical performance metrics. By examining embedding spaces, structural relationships, and feature similarities, we can evaluate the extent to which the student model captures the essential patterns and relationships embedded in the teacher's representations.

This section provides a detailed visual analysis, focusing on embedding space visualization as a critical dimension of knowledge transfer. These visualizations not only allow us to verify the alignment between teacher and student models but also uncover deeper nuances in their respective feature representations. Through these analyses, we aim to highlight the strengths and limitations of the

distillation process, offering a comprehensive understanding of the student model's performance. We then present findings from each visualization approach applied to two datasets, IMDB-AW and DBLP, demonstrating how DistillHGNN achieves effective and efficient knowledge transfer.

The t-SNE visualizations illustrate the model's ability to preserve class relationships and structural information. The student model maintains clear class separations, forming well-defined clusters that closely resemble the teacher's representation. The consistent spatial arrangement of classes between the teacher and student embeddings across the IMDB-AW and DBLP datasets, as shown in Fig. 7, indicates effective knowledge transfer while preserving the essential topological structure of the data.

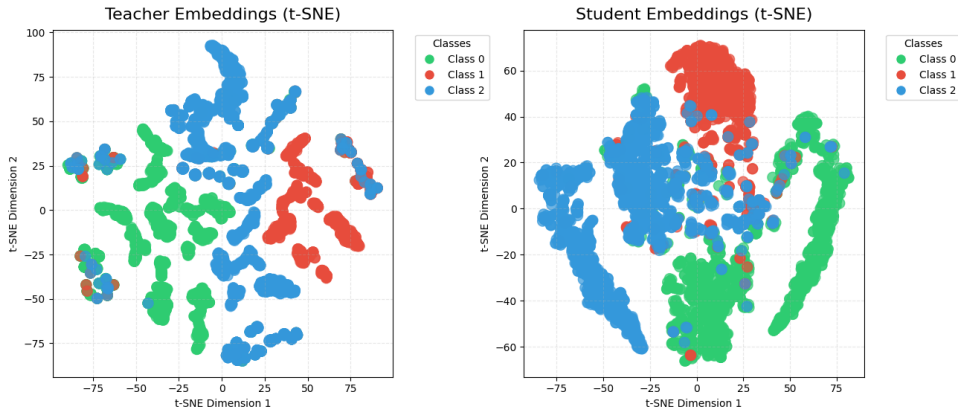

(a) IMDB-AW dataset

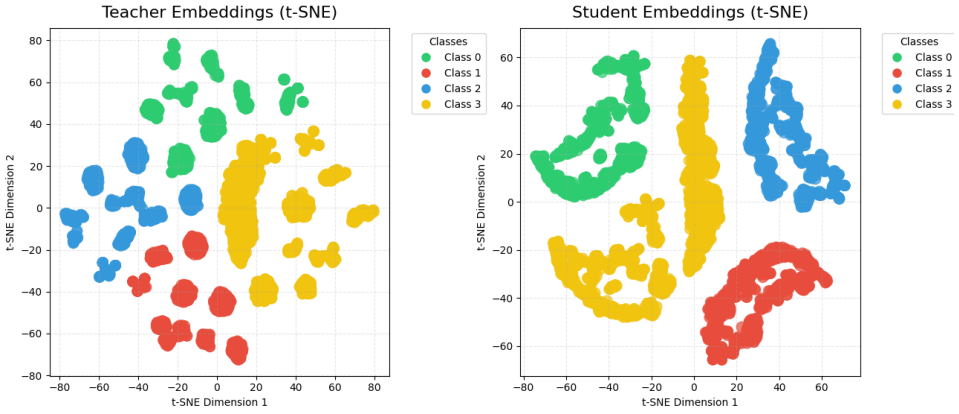

(b) DBLP datasets

Figure 7: t-SNE visualizations comparing teacher and student embeddings for two datasets: (a) IMDB-AW dataset shows scattered and overlapping class distributions in the teacher embeddings, which are effectively refined into cohesive and distinct clusters in the student embeddings, indicating successful knowledge transfer. (b) DBLP dataset reveals fragmented and abnormal class clusters in the teacher embeddings, likely due to the hypergraph model's high-dimensional feature complexities and high-order relationships. In contrast, the student embeddings display well-organized and continuous class regions, demonstrating the effectiveness of knowledge distillation in simplifying and structuring complex representations into interpretable embeddings.

IMDB-AW Dataset Analysis The t-SNE visualization of the IMDB-AW dataset reveals distinct embedding patterns across both models. The teacher model exhibits well-defined clustering for three classes, with Class 2 (blue) showing the most extensive distribution, indicating rich feature diversity within the class. Class 0 (green) demonstrates interesting sub-cluster formations, suggesting un-

derlying structural patterns in the data, while Class 1 (red) maintains moderate cohesion with clear boundaries. The student model successfully preserves these fundamental class relationships while introducing its own structural interpretations. Notably, it maintains class separability while showing a more continuous distribution pattern, with Class 2 adopting an elongated formation and Class 0 demonstrating enhanced cluster cohesion. The slight increase in inter-class mixing, particularly visible in Class 1's boundaries, suggests a balanced trade-off between feature preservation and model simplification.

DBLP Dataset Analysis In the DBLP dataset, both models demonstrate sophisticated four-class separation patterns with distinct characteristics. The teacher model establishes clear class boundaries with unique spatial distributions: Class 0 (green) exhibits multiple sub-clusters in the upper region, indicating complex internal structure; Class 1 (red) forms compact, well-isolated clusters; Class 2 (blue) shows concentrated distribution on the left; and Class 3 (yellow) presents an elongated central formation. The student model transforms this representation into a more globally coherent structure, organizing the classes in a distinctive crescent-like pattern. This arrangement maintains clear class separation while achieving smoother transitions between clusters. The student's representation demonstrates particular effectiveness in boundary definition, with each class occupying a specific region: Class 0 forms a curved structure in the upper left, Class 1 maintains concentration in the lower right, Class 2 shows compact clustering in the upper right, and Class 3 creates a central curved formation.

Both datasets demonstrate successful knowledge transfer between teacher and student models, with the student model consistently achieving more regularized and structured representations. In the IMDB-AW case, the preservation of three-class separation with modified spatial arrangements indicates effective feature learning while maintaining essential data relationships. The DBLP visualization further reinforces this finding across four classes, where the student model's more organized spatial arrangement suggests enhanced feature generalization without loss of discriminative power. These results validate the effectiveness of our knowledge distillation approach, demonstrating that the student model can capture and, in some aspects, enhance the structural understanding of the data despite its simplified architecture.

These visual analyses provide strong empirical evidence for the success of our knowledge distillation framework. The student model's ability to maintain clear class separation while developing more structured representations suggests effective compression of the teacher's knowledge into a more efficient form. This is particularly noteworthy given the architectural simplification, indicating that our approach successfully preserves essential feature relationships while reducing model complexity.

H Related Works

Hypergraph Neural Networks (HGNN). HGNNs extend traditional graph neural networks (GNNs) by capturing complex high-order interactions among multiple nodes through hypergraphs Antelmi et al. (2023). Unlike conventional graphs, where edges connect only two nodes, hypergraphs allow hyperedges to connect multiple nodes, making HGNNs particularly effective in domains where higher-order relationships are crucial Wu et al. (2022). Early models like HGNN Feng et al. (2019) and HpLapGCN Fu et al. (2019) utilized the hypergraph Laplacian matrix for efficient representation learning by smoothing node features across hyperedges. HyperGCN Yadati et al. (2019) further simplified hypergraphs into conventional graphs, applying established GNN techniques to learn node representations, thus leveraging the structural richness of hypergraphs. In addition to spectral approaches, spatial-based hypergraph convolution methods have emerged to overcome earlier limitations. For instance, Bai et al. Bai et al. (2021) introduced a vertex-hyperedge attention mechanism that enhances the focus on critical node-hyperedge interactions. Research such as Yan et al. (2024); Jiang et al. (2019); Yin et al. (2022); Hayat et al. (2024) has explored dynamic hypergraph construction, allowing for flexible representations that adapt to specific datasets. Innovations like two-stage message-passing strategies proposed by Gao et al. Gao et al. (2022), Dong et al. Dong et al. (2020), and Ruggeri et al. Ruggeri et al. (2024) have enabled more efficient information flow across nodes and hyperedges. These advancements have broadened the application of HGNNs, allowing them to effectively model intricate, higher-order relationships in diverse fields

such as social networks, recommendation systems, and biological networks. By capturing complex interactions, HGNNs outperform traditional GNNs, which are limited to pairwise interactions.

Distillation from GNNs and HGNNs to MLPs. Knowledge distillation involves transferring knowledge from a larger, more complex model (the teacher) to a smaller, more efficient model (the student). Previous distillation methods, such as GLNN Zhang et al. (2021) and NOSMOG Tian et al. (2022), primarily use the prediction distribution of teacher GNNs as soft labels to guide student MLPs. However, these approaches often fail to consider the original graph's structure, limiting their ability to capture intricate relationships within the data. For example, while Yang et al. Yang et al. (2021) extracts knowledge from a trained GNN model and transfers it to a student model for more efficient predictions, the method still lacks full integration of structural information into the distillation process. KRD Wu et al. (2023) improves this by quantifying each vertex's knowledge and considering its proximity to neighbors, but it remains limited to low-order graph structures. Additionally, Liu et al. Liu et al. (2022) introduced the HIgh-order RElational (HIRE) knowledge distillation framework for heterogeneous graphs, which captures both first- and second-order information using soft labels. For HGNN-to-MLP distillation, Feng et al. Feng et al. (2024) proposed the LightHGNN model, which incorporates reliable hyperedges to support high-order relations in the distillation process. However, they still relied on soft labels. Similarly, Yu et al. Yu et al. (2024) developed a method to distill knowledge from meta-paths into hypergraphs in heterogeneous graphs, again using soft labels for transferring knowledge from the teacher to the student. This paper aims to address the limitations of prior methods by focusing on hypergraph neural networks (HGNNs). The key challenge in earlier techniques is that soft labels alone do not capture the high-order dependencies inherent in hypergraphs.